

# Pulsating Torque & Electromagnetic Field Analysis for Induction Machine using ANSYS simulation

T.Vignesh<sup>1</sup>, V.Dileepan<sup>2</sup>, P.Kannappar<sup>3</sup>, R.Manoj Babu<sup>4</sup>, P.Elavarasan<sup>5</sup>

<sup>1</sup>Assistant Professor/EEE, Jay Shriram Group of Institutions, Tirupur.

<sup>2,3,4 & 5</sup>UG Scholar/EEE, Jay Shriram Group of Institutions, Tirupur.

## Abstract:

This paper describes an electromagnetic field analysis of the induction machine and pulsating torque. Analyzed machine is three phase induction machine with squirrel cage. Fourier transform is used for the high harmonic components evaluation of the pulsating torque and the magnetic flux density along the air gap. The comparison between computed and measured torque is presented in conclusion. The electromagnetic field analysis is done by the ANSYS simulation. Fourier transform is used for the high harmonic components evaluation of the pulsating torque. The comparison between computed and measured torque is presented in conclusion. Whole experimental measurement was made with measurement card NI PCIe-6361 and shaft DATAFLEX22/20.

**Keywords** — AC machines, electromagnetic analysis, Fourier transform, high harmonic, magnetic fields, measurement torque.

## I. INTRODUCTION

THE magnetic field is possible to resolve to the high harmonic series incurred from concentrated winding in the slots, air-gap inequality due to the slotting. Each of these fields could generate additional torque on the rotor at variable speed at start up. A well-known method to reduce the harmonic content in the line current when operating a grid-commutated inverter is to use a twelve-pulse convertor and a three-winding transformer. This method could be modified and applied in convertor applications with induction machine [5]. When a three phase inverter supplied conventional source to the three phase squirrel cage induction motors exhibit harmonic pulsating of torque. These torque pulsations attain objectionable values during low frequency and in many cases dictate the satisfactory lower limit speed. In industrial applications, uniform speed of rotation these pulsating torques need to be minimized. The results of minimizing the sixth harmonic pulsating torque component in an inverter induction motor drive system using a modified version of Rosenbrock's hill climb technique are presented in [6].

Air gap permeance pulsation caused by rotor slot [7], [16] and stator slot opening is discussed in [1] and [15]. Detection of these harmonics is, of course, a separate issue that depends on number of rotor, stator slots, pole pair numbers, eccentricity, etc. [17]. These slot harmonics are the source of a no negligible part of the unbalanced magnetic pull where the skewing reduces their amplitude. Simulation including slots effect is performed on three phase motor with

36 stator slot, 28 rotor bars, four-pole and with double layer lap winding in [2]. In a multiphase system, here assumed to be a system that comprises more than the conventional three phases. The presence of detrimental spatial harmonics in the air-gap at low speed and start-up is solved in [13]. Main target was reduced copper loss and in addition general expression for the harmonic fields by machine of more than three phases.

The same target for three-phase motor is presented in [8] where Tassarolo and col. designed stator coil for adjusting air-gap space harmonics. Eleven-phase machine which can be excited with harmonics up to the ninth is excited in [14]. The technique is assessed using finite element analysis. Magnetic flux harmonic reduction, torque pulsations minimization, and on the power ratings is presented in [3] and [4] for six-phase induction motor.

Renato O. C. Lyra and Thomas A. Lipo describes a technique of injecting third harmonic zero sequence current components in the phase current. This phase current improves the machine torque density greatly. During starting, Some simple control strategies have been proposed to keep the current constant at any preset value. At starting torque pulsations to eliminate supply frequency [9].

This paragraph deals with the other possibilities of harmonic analysis squirrel cage induction machine. M. Aiello, A. Cataliotti, S. Nuccio measured speed on induction machine based on Chirp-Z transformation (Fig.1) as supply current harmonic analysis [11]. The speed is evaluated from rotor frequency harmonics of

the rotor slots. Authors experimentally results compared with FFT the method is shown on case of 7.5kW induction motor.

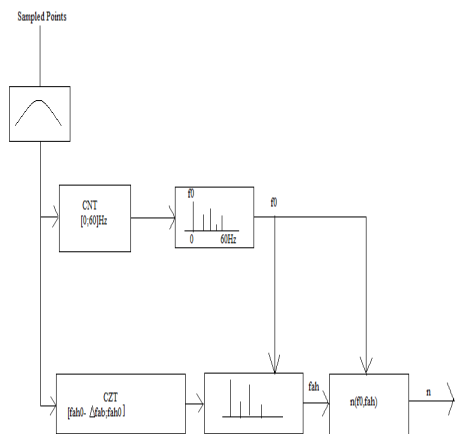


Fig.1. Block diagram of “double Chirp Z Transform algorithm” for induction motor speed measurement based on rotor slot harmonics [11].

## II. TORQUE AND ELECTROMAGNETIC FIELD ANALYSIS

This part is dedicated onto the basic information about analyzed machine. After that follows the electromagnetic field and the torque analysis is done for nominal slip. Analyzed machine is 3-phase induction machine with squirrel-cage, type 1LA7083-2AA10 with power 1.1kW

### A.Parameters of Analyzed Machine

Stator and rotor machine packet is consists from 116 electrical sheet M800–65A, thickness 0.65mm. Winding is placed at the stator U–slots with these parameters: wire diameter 0.64 mm, one parallel wire, one parallel branch, 83 conductors in slot and 6 outlets. The rotor V–slots are filled with aluminum bars on both sides associated of the conductive rings. The stator bore is 64mm and the split ratio of this machine is 0.512. Analyzed machine was design for the following parameters: power 1100W; phase voltage 240V; nominal torque 3.87Nm; frequency 50Hz; nominal current 2.5A; nominal speed 2845rpm; efficiency 77.8% and power factor 0.86.

### B. Electromagnetic Field and Torque Calculation

This part is dedicated to the electromagnetic field

calculation by FEM in the ANSYS program – calculates torque on a body in a magnetic field (command TORQ2D; TORQC2D), with the aid [12].

TORQ2D invokes an ANSYS macro which calculates mechanical torque on a body in form of a magnetic field. The air (symmetry permitted), and a closed path passing through the air elements surrounding the body must be available. A counterclockwise ordering of nodes on the PPATH command will give the correct sign on the torque result. This macro is valid for 2-D planar analysis.

TORQC2D is used for a circular or cylindrical body such as a rotor in an electric machine. The air elements surrounded the body must centered global origin. The air elements covered the path at radius RAD selected. To using the macro, elements with a high permeability material should be unselected prior. This macro is valid for 2-D planar analyses only. The macro calculates the time to average torque, it is done in a harmonic analysis. Radial symmetry model is not necessary at a full 360°.

Meshing problems are common in electrical engineering, and are essentially caused by two factors – the complex geometry of the electro-technical application and the strong variations in the distribution of state variables in certain physical cases.

Sometimes, it is difficult to decide if a new formulation, numerical tool or meshing algorithm will be the optimum means to eliminate the problem. Thus, it appears more judicious to evaluate all the problems by topics and to present their solutions, either by meshing techniques, or by numerical or mathematical techniques. The following topics continually appear – magnetic air gap, movement of conducting materials under a magnetic field, boundary layers, deformations under the effect of electromagnetic forces, magnetic saturation and finally the magnetic field at the infinite. All topics are described in [10].

The electromagnetic torque is being investigated at rated

slip area. The size of the magnetic circuit oversaturation achieved about 1% (Fig. 2), which means percentage of magnetic circuit where is magnetic flux density greater than 1.8T. Behavior of magnetic flux density along the air gap is shown at Fig.3 with average value 0.595T.

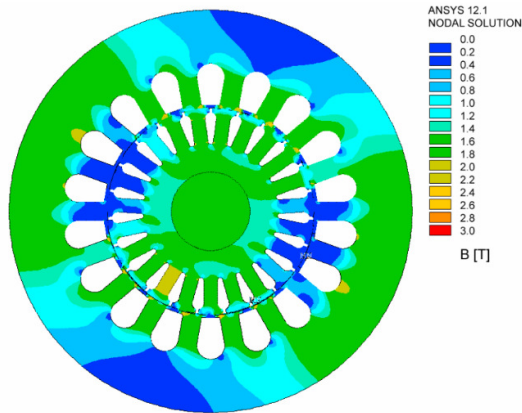


Fig. 2 Electromagnetic field distribution (nominal slip).

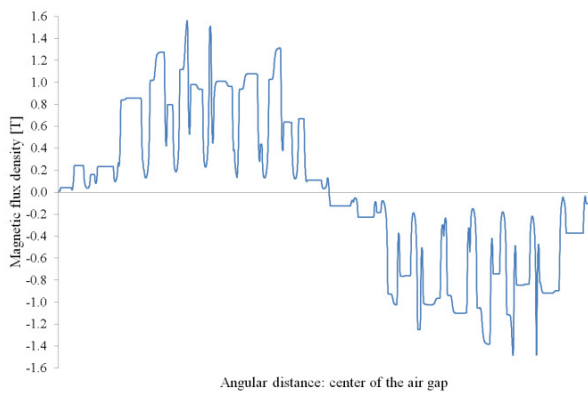


Fig. 3 Behavior of magnetic flux density along the air gap (center).

For this case is electromagnetic torque 3.93Nm. The results of spectral analysis are shown at Fig. 4. There is a noticeable increase in slot harmonics of the magnetic flux density. The size of the electromagnetic torque pretty well describes the torque characteristic (Fig. 5), especially around the operating point of the machine. Positive sign of torque represents operating mode for motor and negative sign of torque represents operating mode for generator.

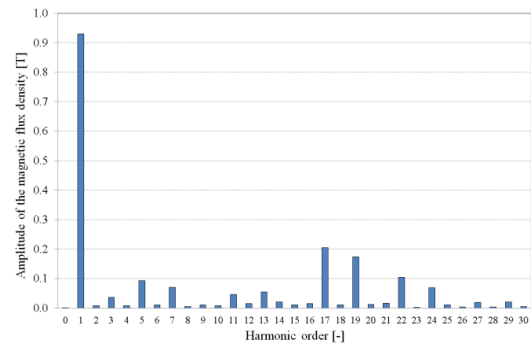


Fig. 4 High harmonic components of magnetic flux along the air gap.

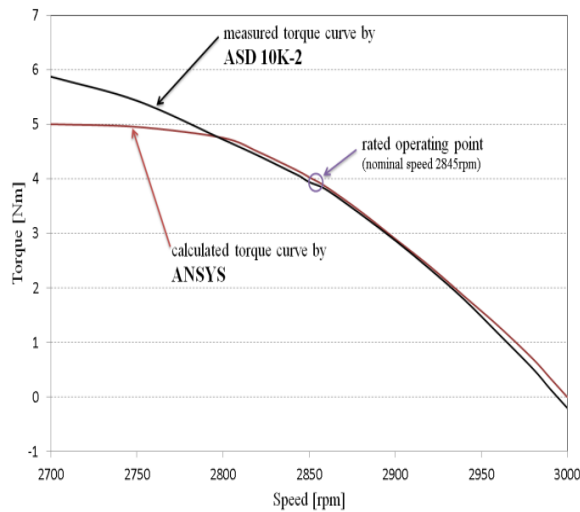


Fig. 5 Torque comparison – measured vs. calculated (ANSYS).

The torque is calculated via a circular path integral of the Maxwell stress tensor. Fourier transform is used for high harmonic components evaluation of calculated pulsating torque behavior (Fig. 6). In conclusion the comparison between computed pulsating torque and measured pulsating torque along the one rotor turn is presented.

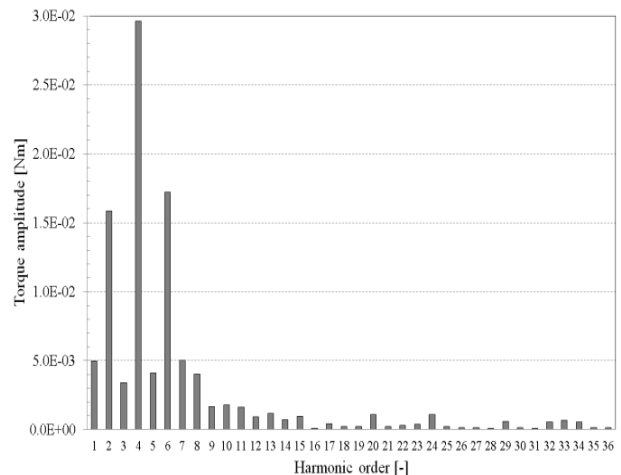


Fig. 6 High harmonic torque components from electromagnetic field.

In the spectrum of pulsating torque are included higher- order spatial harmonics, with dc component 3.9Nm. All is done for nominal load (slip is 5.17%).

### III. TORQUE MEASUREMENT

The torque measurement is divided onto the three parts: mechanical torque measurement, dynamic torque measurement at start up and pulsating torque measurement in case of the nominal load (nominal slip).

### A. Mechanical torque

The load characteristic was measured for slip in range from 0 up to 10%. Based on these measurements can be gradually set the parameters of the equivalent circuit and thereby obtain the necessary input for electromagnetic analysis. Behavior of the mechanical torque and stator phase current is shown at the following figure (Fig. 7), where the nominal mechanical torque, the nominal speed (slip) and the nominal current is marked, see figure.

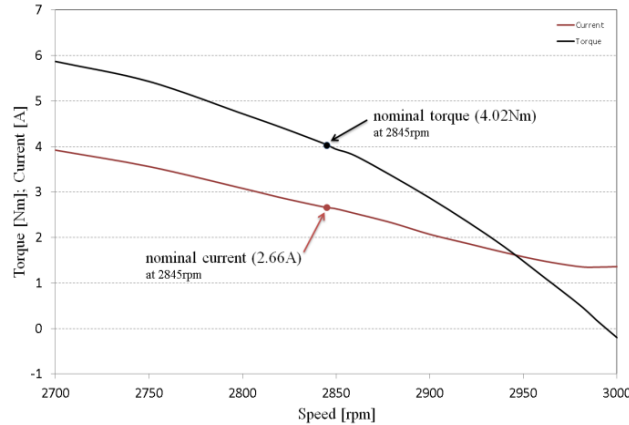


Fig. 7 Behavior of the mechanical torque and stator current.

### B. Additional torque and the speed characteristic during the machine start-up process

Experimental measurement was made with measuring card NI PCIe-6361 (Fig. 1) and shaft DATAFLEX 22/20 (Fig. 2). The results of experimental measurement (Fig. 8)(the engine was loaded with inertia torque of the flywheel  $J_{FV}=0.0182\text{kg.m}^2$ ) are processed in LabVIEW. Self-inertia torque of analyzed machine is  $0.0011\text{kg.m}^2$ . The results of the start-up torque measurement and the speed characteristic are shown in the following graphs (Fig. 9-10). The torque characteristic with marking of area, where additional asynchronous torque occurs is shown on the Fig. 9. The maximal dynamic start-up torque and both torque envelope are also marked in the following figure.

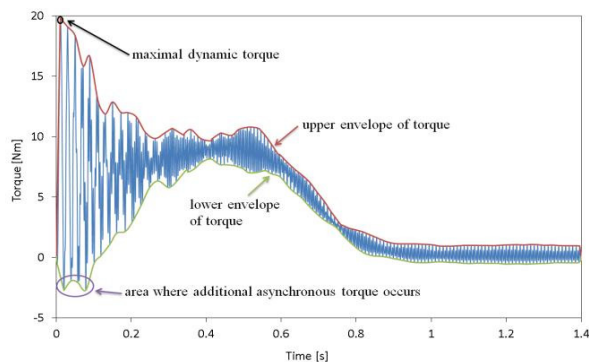


Fig. 8 Mechanical torque during the machine start-up with flywheel.

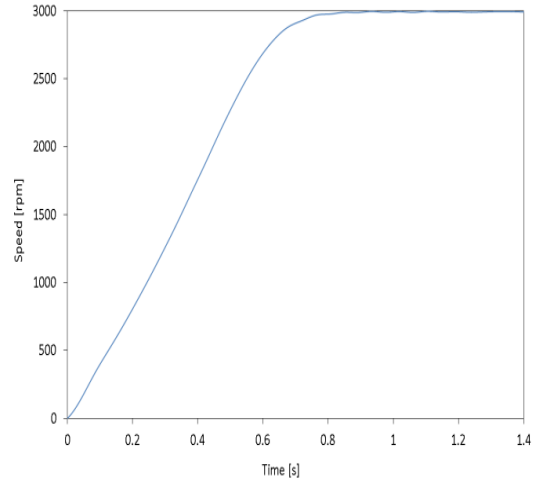


Fig. 9 Speed characteristic during the machine start-up with flywheel

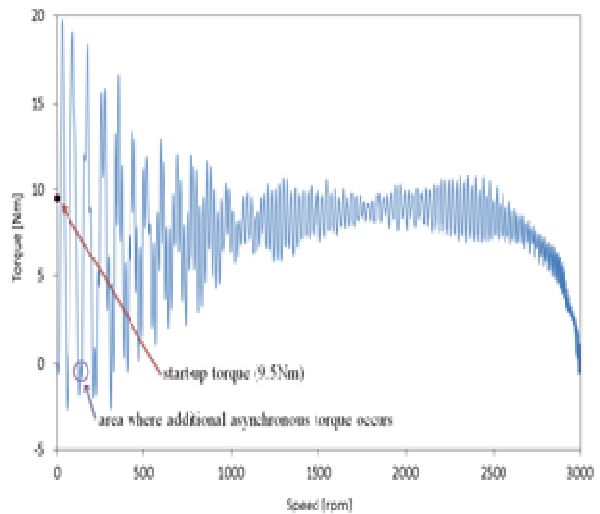


Fig. 10 Torque characteristic during the machine start-up.

The looked-rotor torque value was measured as a multiple of the nominal torque  $MZ=2.45MN$  which corresponding with manufacturer tolerance – according to the manufacturer's (Fig. 11) the looked-rotor torque is in range  $MZ=(1.9-2.6)MN$ .

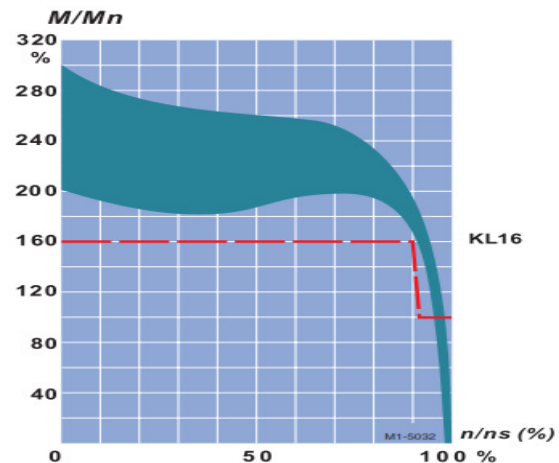


Fig. 11 Diagram of the torque characteristic classification..

C. Pulsating torque at steady-state

The pulsating torque measurement (Fig. 12) was made with the following condition: steady-state with nominal load (it means the load torque 3.87Nm). High harmonic components of pulsating torque are shown at the Fig. 9, where the dc component is 3.91Nm.

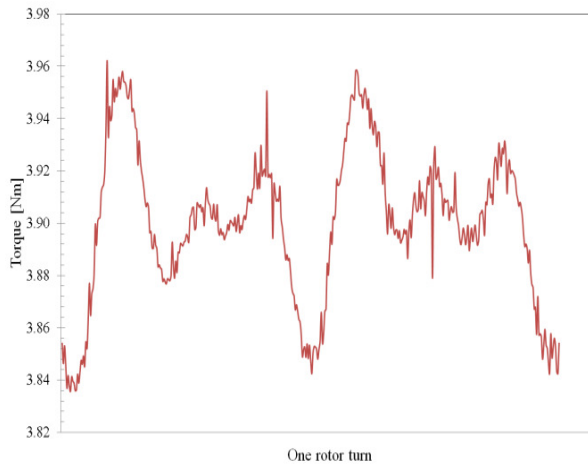


Fig. 12 Pulsating torque per one rotor turn (at steady-state).

IV .CONCLUSION

Analyzed machine is 3-phase induction machine with squirrel-cage rotor 1LA7083-2AA10 with power 1.1kW. Typically, these machines are used as drive of industrial applications, etc. fans, pumps, machine tools, press and others. The load characteristic was measured for slip in range from 0 up to 10%. Based on these measurements can be gradually set the parameters of the equivalent circuit (classical “T-cell” it was used) and thereby obtain the necessary input for electromagnetic analysis.

Analyzed machine is 3-phase induction machine. Typically, these machines are used as drive of industrial applications, etc. fans, pumps, machine tools, press and others. The load characteristic was measured for slip in range from 0 up to 10%. Based on these measurements can be gradually set the parameters of the equivalent circuit (classical “T-cell” it was used) and thereby obtain the necessary input for electromagnetic analysis.

The results of experimental measurement of the torque at the start-up were processed in the LabVIEW program. The comparison of the experimental measurement results and calculation results (from the Maxwell program) is done at the following figures, Fig.13-16.

Finally, from the electromagnetic field the pulsating torque behavior per one complete turn of rotor and then high harmonic torque components were calculated. The spectral analysis results of the magnetic flux density along the air gap has been done and also the pulsating torque along the air gap. The resultant pulsating torque is out of its DC component consists of higher orders spatial harmonics. Course pulsating torque obtained retrospectively from the electromagnetic field is different from the measured. This is due to the fact that the analysis was not possible to cover all the things that affect the pulsating torque value and the higher spatial harmonics creation. For the calculation of

pulsating torque the model should be adjusted (see comparison on Fig. 13). The dc components are practically the same, but the differences between measurement and calculation are apparent and they are caused by the model simplification

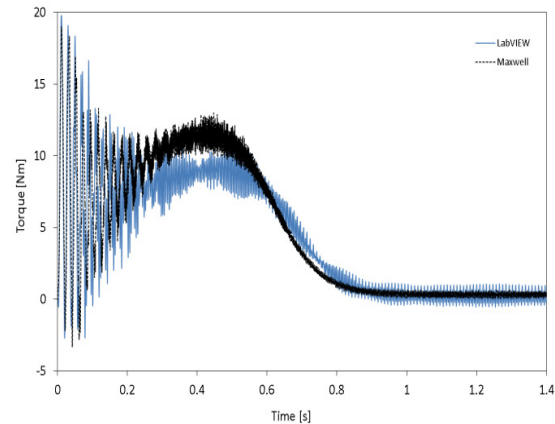


Fig. 13 Comparison of the torques during the analyzed machine start-up.

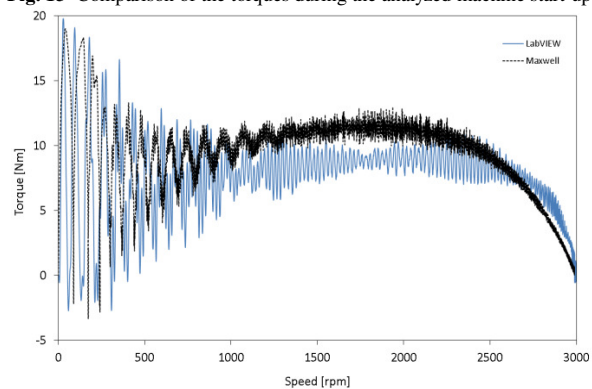


Fig. 14 Comparison of the torque characteristics of the analyzed machine.

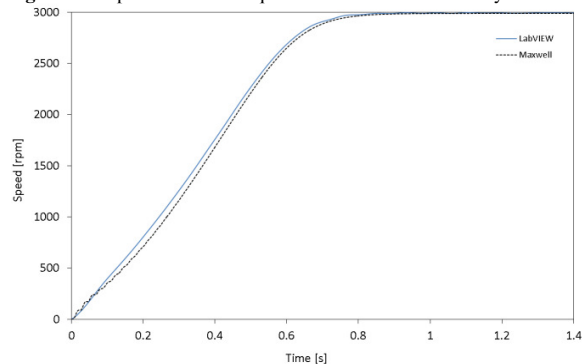


Fig. 15 Comparison of the speed characteristics of the analyzed machine.

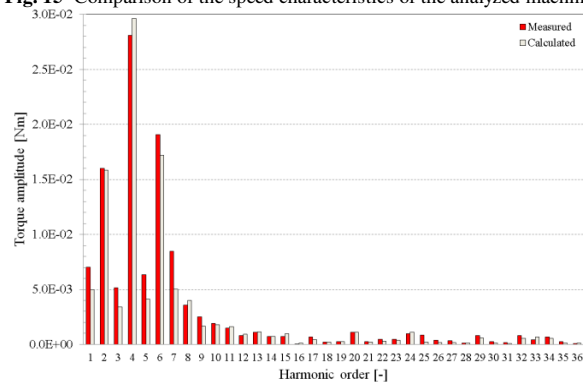


Fig. 16 High harmonic components comparison of pulsating torques –



measurement and calculation

## Reference:

- [1] Frauman, P.; Burakov, A.; Arkkio, A.; , "Effects of the Slot Harmonics on the Unbalanced Magnetic Pull in an Induction Motor With an Eccentric Rotor," *Magnetics, IEEE Transactions on* , vol.43, no.8, pp.3441-3444, Aug. 2007 doi: 10.1109/TMAG.2007.899470
- [2] Nandi, S.; , "Modeling of induction machines including stator and rotor slot effects," *Industry Applications Conference, 2003. 38th IAS Annual Meeting. Conference Record of the* , vol.2, no., pp. 1082-1089 vol.2, 12-16 Oct. 2003 doi: 10.1109/IAS.2003.1257684
- [3] Lyra, R.O.C.; Lipo, T.A.; , "Torque density improvement in a six- phase induction motor with third harmonic current injection," *Industry Applications Conference, 2001. Thirty-Sixth IAS Annual Meeting. Conference Record of the 2001 IEEE* , vol.3, no., pp.1779-1786 vol.3, 30 Sep-4 Oct 2001 doi: 10.1109/IAS.2001.955773
- [4] Lyra, R.O.C.; Lipo, T.A.; , "Torque density improvement in a six- phase induction motor with third harmonic current injection," *Industry Applications, IEEE Transactions on* , vol.38, no.5, pp. 1351- 1360, Sep/Oct 2002 doi: 10.1109/TIA.2002.802938
- [5] J. Hylander, S. von Zwegbergk, "Induction machines with two three- phase windings in converter applications", *IEEE Trans. Industry and General Applications*, pp. 173 – 176, 1989.
- [6] T.V. Avadhanlu, R.B. Saxena, "Torque Pulsation Minimization in a Variable Speed Inverter-Fed Induction Motor Drive System", *IEEE Trans. Power Apparatus and Systems*, Issue 1, pp. 13 – 18, 1979, 10.1109/TPAS.1979.319504.
- [7] Keysan, O.; Bulent Ertan, H.; , "Higher order rotor slot harmonics for rotor speed & position estimation," *Optimization of Electrical and Electronic Equipment (OPTIM), 2010 12th International Conference on* , vol., no., pp.416-421, 20-22 May 2010 doi: 10.1109/OPTIM.2010.5510487
- [8] Tessarolo, A.; Mezzarobba, M.; Contin, A.; , "A stator winding design with unequally-sized coils for adjusting air-gap space harmonic content of induction machines," *Electrical Machines (ICEM), 2010 XIX International Conference on* , vol., no., pp.1-7, 6-8 Sept. 2010 doi: 10.1109/ICELMACH.2010.5608286
- [9] Zenginobuz, G.; Cadirci, I.; Ermis, M.; Barlak, C.; , "Soft starting of large induction motors at constant current with minimized starting torque pulsations," *Industry Applications, IEEE Transactions on* , vol.37, no.5, pp.1334-1347, Sep/Oct 2001 doi: 10.1109/28.952509
- [10] G. Meunier: *The Finite Element Method for Electromagnetic Modeling*. Published by ISTE Ltd and John Wiley & Sons, Inc., Great Britain, 2008, ISBN: 978-1-84821-030-1.
- [11] Aiello, M.; Cataliotti, A.; Nuccio, S.; , "An induction motor speed measurement based on current harmonic analysis with Chirp-Z Transform," *Instrumentation and Measurement Technology Conference, 2001. IMTC 2001. Proceedings of the 18th IEEE* , vol.1, no., pp.578-582 vol.1, 21-23 May 2001 doi: 10.1109/IMTC.2001.928884
- [12] Release 10.0 Documentation for ANSYS Manual.
- [13] Williamson, S.; Smith, S.; , "Pulsating torque and losses in multiphase induction machines," *Industry Applications, IEEE Transactions on* , vol.39, no.4, pp. 986-993, July-Aug. 2003 doi: 10.1109/TIA.2003.813722
- [14] Abdel-Khalik, Ayman S.; Masoud, Mahmoud. I.; Williams, B. W.; , "Optimum flux distribution with harmonic injection for multiphase induction machine," *Power Electronics, Machines and Drives (PEMD 2010), 5th IET International Conference on* , vol., no., pp.1-6, 19-21 April 2010 doi: 10.1049/cp.2010.0106
- [15] Ishizaki, A.; Liang, G.; Saitoh, K.; , "Quantitative study on harmonic flux densities of squirrel-cage induction motors," *Magnetics, IEEE Transactions on* , vol.26, no.2, pp.956-959, Mar 1990 doi: 10.1109/20.106477 [16] Nandi, S.; , "Slot permeance effects on rotor slot harmonics in induction machines," *Electric Machines and Drives Conference, 2003. IEMDC'03. IEEE International* , vol.3, no., pp. 1633- 1639 vol.3, 1-4 June 2003 doi: 10.1109/IEMDC.2003.1210670
- [16] Nandi, S.; , "Slot permeance effects on rotor slot harmonics in induction machines," *Electric Machines and Drives Conference, 2003. IEMDC'03. IEEE International* , vol.3, no., pp. 1633- 1639 vol.3, 1-4 June 2003 doi: 10.1109/IEMDC.2003.1210670
- [17] Nandi, S.; Ahmed, S.; Toliyat, H.A.; , "Detection of rotor slot and other eccentricity related harmonics in a three phase induction motor with different rotor cages," *Energy Conversion, IEEE Transactions on* , vol.16, no.3, pp.253-260, Sep 2001 doi: 10.1109/60.937205